AD-A167 127 ARGON PUFF GAS SOFT X-RAY LASER(U) NAVAL RESEARCH LAB 1/1
WASHINGTON DC J DAVIS ET AL. 25 APR 86 NRL-MR-5771

UNCLASSIFIED F/G 20/5 NL

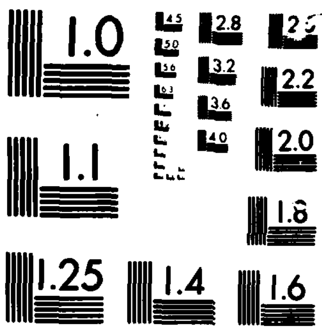

MICROCOP CHART

NRL Memorandum Report 5771

Argon Puff Gas Soft X-Ray Laser

J. DAVIS, J. P. APRUZESE, C. AGRITELLIS* AND P. KEPPLE

Plasma Radiation Branch
Plasma Physics Division

**Science Applications International Corporation*
McLean, VA 22102

April 25, 1986

This work was supported in part by the Strategic Defense Initiative Organization and the Defense Nuclear Agency under Subtask QIEQMXLA, work unit 00006 and work unit title "XRL Source."

NAVAL RESEARCH LABORATORY
Washington, D.C.

Approved for public release; distribution unlimited.

DISCLAIMER NOTICE

SECURITY CLASSIFICATION OF THIS PAGE

REPORT DOCUMENTATION PAGE

1a. REPORT SECURITY CLASSIFICATION UNCLASSIFIED	1b. RESTRICTIVE MARKINGS
2a. SECURITY CLASSIFICATION AUTHORITY	3. DISTRIBUTION/AVAILABILITY OF REPORT Approved for public release; distribution unlimited.
2b. DECLASSIFICATION / DOWNGRADING SCHEDULE	
4. PERFORMING ORGANIZATION REPORT NUMBER(S) NRL Memorandum Report 5771	5. MONITORING ORGANIZATION REPORT NUMBER(S)
6a. NAME OF PERFORMING ORGANIZATION Naval Research Laboratory 6b. OFFICE SYMBOL (If applicable) Code 4720	7a. NAME OF MONITORING ORGANIZATION
6c. ADDRESS (City, State, and ZIP Code) Washington, DC 20375-5000	7b. ADDRESS (City, State, and ZIP Code)
8a. NAME OF FUNDING/SPONSORING ORGANIZATION Defense Nuclear Agency 8b. OFFICE SYMBOL (If applicable) RAEV	9. PROCUREMENT INSTRUMENT IDENTIFICATION NUMBER
8c. ADDRESS (City, State, and ZIP Code) Alexandria, VA 22310	10. SOURCE OF FUNDING NUMBERS PROGRAM ELEMENT NO. 62715H; PROJECT NO. 85-677; TASK NO.; WORK UNIT ACCESSION NO. DN155-166

11. TITLE (Include Security Classification)
Argon Puff Gas Soft X-Ray Laser

12. PERSONAL AUTHOR(S)
Davis, J., Apruzese, J. P., Agritellis, C.* and Kepple, P.

13a. TYPE OF REPORT	13b. TIME COVERED	14. DATE OF REPORT (Year, Month, Day)	15. PAGE COUNT
Interim	FROM ______ TO ______	1986 April 25	39

16. SUPPLEMENTARY NOTATION
*Science Applications International Corporation, McLean, VA 22102 (Continues)

17. COSATI CODES			18. SUBJECT TERMS (Continue on reverse if necessary and identify by block number)
FIELD	GROUP	SUB-GROUP	X-Ray laser; Implosion
			Gas puff; Non-LTE

19. ABSTRACT (Continue on reverse if necessary and identify by block number)

A non-LTE dynamic argon pinch model has been applied to investigate the feasibility of creating conditions favorable to gain coefficients in excess of unity during the implosion of a cylindrical annular argon gas puff plasma. Preliminary results obtained from the SIMPLODE model suggest that it is possible to achieve measureable gain in the 3p-3s lasing transition at 434 Å in neonlike argon.

20. DISTRIBUTION/AVAILABILITY OF ABSTRACT ☒ UNCLASSIFIED/UNLIMITED ☐ SAME AS RPT. ☐ DTIC USERS	21. ABSTRACT SECURITY CLASSIFICATION UNCLASSIFIED
22a. NAME OF RESPONSIBLE INDIVIDUAL Jack Davis	22b. TELEPHONE (Include Area Code) (202) 767-3278 22c. OFFICE SYMBOL Code 4720

DD FORM 1473, 84 MAR — 83 APR edition may be used until exhausted. All other editions are obsolete. — SECURITY CLASSIFICATION OF THIS PAGE

16. SUPPLEMENTARY NOTATION (Continued)

This work was supported in part by the Strategic Defense Initiative Organization and the Defense Nuclear Agency under Subtask QIEQMXLA, work unit 00006 and work unit title "XRL Source."

CONTENTS

ARGON PUFF GAS SOFT X-RAY LASER

I. Introduction

The successful demonstration of soft x-ray lasers[1-5] using as the lasing medium the plasma generated from high power laser-target interaction has provided considerable impetus to a number of alternative techniques for producing an x-ray laser. One such scenario involves the application of pulse power drivers to implode gas puff plasmas. Of the many variations in the target design there are three basic concepts currently under investigation. They are: (1) a single cylindrical annular gas puff, (2) a single cylindrical annular gas puff imploding on a central core plasma, and (3) similar to (1) and (2) except that the imploded plasmas are not the lasing medium but a source of intense x-ray emission for photopumping a target material. Scenarios (2) and (3) are discussed by the authors and by T. Hussey elsewhere.[6,7] Since the single gas puff plasma is central to all three scenarios, it is essential that we understand fully its radiative properties and behavior. Therefore, the focus of this investigation will be confined to the dynamics of a single gas puff plasma. The intent here is to concentrate on the radiation kinetics while characterizing the implosion dynamics of the gas puff plasma by means of the simplest plausible description, i.e., a dynamic pinch model. Obviously, such a model ignores much of the observed pathological behavior of these plasmas, but it does provide a starting point for determining whether it is at all feasible to produce temperature and

Manuscript approved January 16, 1986.

density conditions favorable to x-ray lasing. The influence of the development and growth of plasma instabilities and their impact on the uniformity and homogeneity of the evolving plasma is a critical issue and is currently under investigation. Preliminary results based on 2-D Magneto-Radiation-Hydrodynamic simulations and experiments,[8] employing plasma erosion switches, suggest a significant reduction in the role of instabilities and provides encouragement for further pursuit of this design.

The treatment presented here is based on a simple model, hereafter referred to as SIMPLODE, with emphasis on the atomic kinetics and radiation dynamics self-consistently coupled to a dynamic pinch model in order to obtain information on the plasma environment as it evolves under the influence of the current discharge. This provides us with a self-consistent picture of temperature, density, size, and level population during the plasma's evolution. The influence of radiation transport on the level inversion and gain calculations is taken into account using Sobolev's method.[9,10] In either a stationary medium or one moving without velocity gradients, the final emission of optically thick line photons or continuum from the medium generally occurs from unit optical depth from the boundary. Photons originating deep in the interior of the medium undergo successive scatterings on their flight to the surface before escaping. In this instance the emitted radiation reflects nonlocal conditions. On the other hand, if the medium has a velocity gradient then radiation originating deep in the interior of the plasma can escape the medium directly because of the Doppler effect and this radiation reflects the local interior conditions rather than conditions at other points in the medium and, in particular, the boundary. This is the essence of Sobolev's approximation. A more thorough discussion of the effect of radiation transport on the gain of the lasing transitions can be found in reference

7. Also, since the experiments on the GAMBLE II facility at NRL are being done with an argon gas puff plasma, the theory and analysis presented here is for argon.

So far the discussion has been general focusing on the plasma and its properties. However, in particular, we will investigate the feasibility of creating a population inversion in the 3p levels of neonlike argon due to electron impact collisional excitation from the $2p^6$ ground state and estimate the gain coefficients in the $n=3$, $\Delta n=0$ lasing transitions.

II. Physical Model

The simplest description of an imploding Z-pinch plasma is probably the Bennett Pinch equilibrium model. This model is based on an equilibrium balance between the fluid and magnetic pressures in combination with an equilibrium balance between the sources and sinks of energy. The classical Bennet pinch ignores radiation and hence ignores excitation/ionization energy (chemical potential) and energy lost by radiation (radiation cooling). An obvious extension to the Bennett pinch equilibrium model is the inclusion of the flow parameters describing the temporal evolution of the plasma. That is, maintain the simple philosophy of the Bennett pinch but allow the plasma to radiate and evolve in time. In essence, this is our philosophy - a radiating dynamic Bennett pinch; SIMPLODE. Also, like Shearer,[11] who included a radiation cooling term in the form of Bremsstrahlung losses from a pure hydrogen plasma, we include radiation cooling but in a much more extensive fashion. The radiation cooling term in our model includes contributions from free-free, free-bound, and bound-bound transitions and is determined from a non-LTE collisional-radiative model of the level dynamics.[12]

The SIMPLODE model describes the radial implosion of a cylindrical annular gas puff plasma of uniform density carrying a uniform current in the axial direction. Only radial motion is considered, i.e., there is no axial structure and the plasma is always uniform in this direction. The radial motion is determined from the force equation, vis.

$$m \frac{d^2r}{dt^2} = \left(P - \frac{I^2}{2\pi r^2 c^2}\right) A \tag{1}$$

where r is the radial distance measured from the symmetry axis, P is the fluid pressure, A is the area over which the force is exerted, i.e., $2\pi r\ell$, and $I^2/2\pi r^2 c^2$ is the magnetic pressure, i.e., $B^2/8\pi$. The thermal energy, $E_{th}=3/2\ (1+Z)n_i kT + \Sigma u_p$, varies in time as

$$\frac{dE_{th}}{dt} = -\frac{P}{N}\left(\frac{\dot{V}}{V}\right) + \frac{zI^2}{A_{curr.}}\ell - P_{rad}V \tag{2}$$

where Σu_p is the sum of ionization energies and is loosely referred to as chemical potential. $A_{curr} = \pi(R_B^2-R_A)^2$ where $R_B(R_A)$ represents the outer (inner) radius of the annular plasma, $\dot{V}= 2\pi\ell r\dot{r}$, $N=(m/m_i)/\pi r^2\ell$ where m is the plasma mass, m_i is the atomic mass, $n_i = m/m_i$, and the thermal pressure is $N(1+Z)kT$. Finally, ℓ is the length of plasma, Z is the charge state, z is the classical resistivity, and P_{rad} is the power radiated per unit volume V. The remaining sysmbols have their usual meaning. The first term on the RHS of Eq. (2) represents the work done in compressing the plasma, the second expression is the joule heating source term, and the third term is the power radiated, i.e., radiative cooling.

The collisional-radiative model describing the level dynamics contains an extensive number of levels in the K- and L-shells with particular emphasis on the neonlike ionization stage which contains 42 excited states in j-j representation and 385 lines. The line profile functions are

represented by Voigt functions and include natural and Doppler broadening. The transport of radiation employs the Sobolev escape model.

The "x-ray" lasing scheme considered here takes advantage of the large monopole excitation rate from the ground state to the excited 3p state of the neonlike ionization stage. Although we are focusing on a collisional excitation scheme, all other scenarios, such as recombination lasers, can be investigated with this model. However, by controlling the implosion we hope to avoid burning through the neonlike stage and instead create conditions for producing a stable abundance of neonlike argon. A simplified energy level diagram for neonlike argon is shown in Fig. 1. A population inversion can occur in the 3d and/or 3p levels leading to gain and lasing in the 3d-3p and 3p-3s transitions. This is indicated specifically for the 3p-3s transition with the label L(434Å).

III. Results and Discussion

Preliminary estimates for the neonlike fractional abundance and gain coefficient in a stationary environment were obtained from the collisional-radiative model for prescribed values of temperature, density, velocity, and size. These estimates provide a measure of the parameter space over which gain can be expected as well as providing guidance for the SIMPLODE simulations. In Fig. 2 the neonlike ground state fractional abundance is presented as a function of temperature for several ion densities in the absence of opacity effects, i.e., the optically thin case. For temperatures from about 30 to 70 eV, for densities typical of imploding gas puff plasmas, a significant amount of neonlike argon prevails. The gain coefficient for the 3p-3s transition is shown in Fig. 3, for an optically thin plasma. The gain for a Doppler broadened line is given by

$$\alpha = 10^{-16} f_{osc.} \lambda(A)(M/T)^{1/2}(N_2 - \frac{g_1}{g_2} N_1) \text{ cm}^{-1} . \qquad (3)$$

where $f_{osc.}$ is the absorption oscillator strength of the line, λ is the wavelength in angstroms, M is the atomic mass of the radiating ion, T is the temperature of the plasma in eV, N_2 (N_1) is the upper (lower) level population, and g_i is the statistical weight of level i. The gain coefficient for a Doppler broadened line is directly proportional to the wavelength of the lasing line and the difference between the upper and lower level population densities, and inversely proportional to the square root of the temperature. For an optically thin plasma, gain coefficients greater than unity exist for all three densities over a broad temperture range with a peak gain coefficient of about 30 cm^{-1} at 60 eV for an ion density of $1.5\times10^{19} cm^{-3}$. For a fixed density and increasing temperature the number of neonlike ions decreases due to increased ionization causing burnthrough; for decreasing temperature the plasma becomes too cold to support the existence of neonlike ions, and the collisional excitation rates of the 3p neonlike levels drop drastically. Similarly, for a fixed temperature and increasing density the fractional abundance of neonlike ions decreases due to the increase in the ionization rate causing burnthrough; another way of viewing this situation is to note that as the density increases for a fixed temperature the ionization balance tends toward LTE which causes a given ionization state to appear at a lower temperature than a plasma in collisional-radiative equilibrium.

In Figs. 4 and 5 we have presented results for a optically thick plasma with a diameter of 0.9mm and imploding with a peak velocity of 2×10^7 cm/sec. (These parameters are typical of argon implosions on the GAMBLE II facility.) In this case the neonlike ion fraction starts falling off more rapidly at lower temperature than in the optically thin case. The

differences are greatest for the higher densities due to the combined effects of collisions and the radiation field.

The combined effects of velocity and opacity can but be understood by first considering them separately and then as a composite. In Fig. 6 the results of several calculations are presented for varied conditions while maintaining the total ion density fixed at $5\times10^{17}cm^{-3}$. The optically thin result is included for reference and comparison purposes. The influence of opacity on the production of neonlike ions is shown on the v=0, diameter = 0.9mm curve. In comparison with the optically thin case, it is seen that an increase in plasma size manifests itself with an increase in opacity which maintains the radiation field in the plasma thereby making it easier to achieve a given degree of ionization, in this instance the neonlike stage, at a lower electron temperature than the optically thin case. Therefore, for a fixed electron temperature opacity effects will enhance the plasmas' degree of ionization above that achieved in a purely collisional optically thin plasma. Hence, the rapid decrease in neonlike ions when the plasma is opaque. With increasing temperature collisional ionization will reduce the number of neonlike ions in both cases. The influence of velocity on the neonlike ion fraction can be understood in the following way. In plasmas where the directed motional velocity exceeds the thermal velocity the escape probability is enhanced. In essence, when the line quanta impinge on a region of plasma where the local velocity has shifted the apparent frequency of the line away from the line center, where absorption is greatest, the quanta are able to escape the entire plasma. Therefore, the effects of velocity tend to reduce the effective opacity, associated with a stationary plasma, making the plasma effectively thin. Even though the velocity tends to mitigate the effects of opacity, it does not entirely remove opacity in the regimes considered, but the neonlike fraction does increase in the direction of the optically thin result.

Finally, to explore the effects of mixing elements we have included the results of calculations where 10^{19} neon ions per cm^3 are mixed with $5x10^{17}$ argon ions per cm^3. These results are shown also in Fig. 6 with the consequence of further reducing the number of neonlike argon ions due to increased collisional effects induced by the higher density.

The gain calculations for the conditions depicted in Fig. 6 are shown in Fig. 7. Note the inclusion of an additional gain curve for a velocity of $1x10^7$cm/sec and a diameter of d=0.9mm. For the conditions described in Fig. 7, gain coefficients can be achieved in excess of unity in the 3p-3s lasing transition at 434A for peak implosion velocities in excess of $1x10^7$cm/sec. It is clear from these single plasma calculations that for prescribed values of temperature, density, velocity an size, that are representative of gas puff implosions, it should be possible to create a population inversion and achieve gain coefficients in excess of unity.

We will now investigate whether these conclusions will prevail in a dynamic environment such as that generated by the SIMPLODE model. For illustrative purposes, we present the results of calculations for a reference case of a 4 cm long, 35 ugm/cm argon gas puff plasma distributed uniformly between the outer and inner radius of 1.55 and 0.95 cm, respectively. The driving current waveform typical of the GAMBLE II generator, with the Plasma Erosion Opening Switch, is shown in Fig. 8. Peak current of $8.75x10^5$ amps is attained in about 50 nsec, decaying to about $6x10^5$ amps in another 70 nsec and then falling precipitously to zero in 100 nsec. The temporal behavior of the radiis is shown in Fig. 9. The inner radius collapses and stagnates on axis while the outer radius continues inward until the back pressure is sufficient to impede the forward motion and bounces outward. The final pinch radius is about 1/10 the initial radius and is in good agreement with the bulk of experimental

data accumulated over the years from a variety of generators and plasma loads. The variation of velocity as a function of time, shown in Fig. 10, reaches a peak value of 1.1×10^{7} cm/sec in about 160 nsec which is well after peak current. This behavior is characteristic of the GAMBLE II generator and is especially true of driving currents with sharp risetimes. The implosion phenomenology suggests that the plasma heats up and percolates for a time and then eventually coasts inward. The temporal variations of temperature and density are shown in Figs. 11 and 12, respectively. The ion density peaks at the pinch and reaches a value of 3×10^{18} ions/cm^3 while the peak temperature occurs some 15 nsec earlier and reaches a value of about 165 ev. The total radiative yield which essentially comes from the L-shell, is roughly 1 kilojoule and exhibits a pulse duration of about 25 nsec as shown in Fig. 13. This result is in reasonably good agreement with the experimental observations from GAMBLE II.[8]

A sample of the gain coefficient for the 434 A line is shown as a function of time in Fig. 14 for the illustrative case represented in Figs. 8-12. The gain coefficient was greater than unity for a long time reaching a peak value of about 4 cm^{-1} late in the implosion. The values obtained for the gain coefficient are probably reasonable around peak compression but become less reliable after the bounce because of the lack of an adequate physics description of this late stage. However, it is encouraging that conditions prevail for producing measurable gains over a 4 cm length of plasma assuming, of course, stability of the column. Work is currently in progress using more sophisticated models to assess the validity of our findings here.

Finally, a series of simulations were performed to determine the plasma parameters at maximum gain as a function of M/ℓ for fixed $\Delta r=0.60$ corresponding to $R_B=1.55$ cm and $R_A=0.95$ cm. The ion density and

temperature, at maximum gain, are shown as a function of M/ℓ in Figs. 15 and 16, respectively. The gain coefficient as a function of M/ℓ is shown in Fig. 17. For $\Delta r=0.60$, the gain coefficient peaks at $M/\ell=60\mu gm/cm$ and has a value of about 4 cm^{-1}.

IV. Summary

It has been theoretically demonstrated that it is possible to create conditions favorable to population inversion and gain coefficients in excess of unity for a variety of conditions by imploding a cylindrical annular argon gas puff plasma. Gain coefficients of 4 cm^{-1} have been calculated for the 3p-3s lasing transition in neonlike argon at 434 Å.

Acknowledgments

This work was supported in part by the Strategic Defense Initiative Organization through the Defense Nuclear Agency and by the Office of Naval Research. We would like to thank Drs. F. Young and S. Stephanakis for making the experimental results available prior to publication.

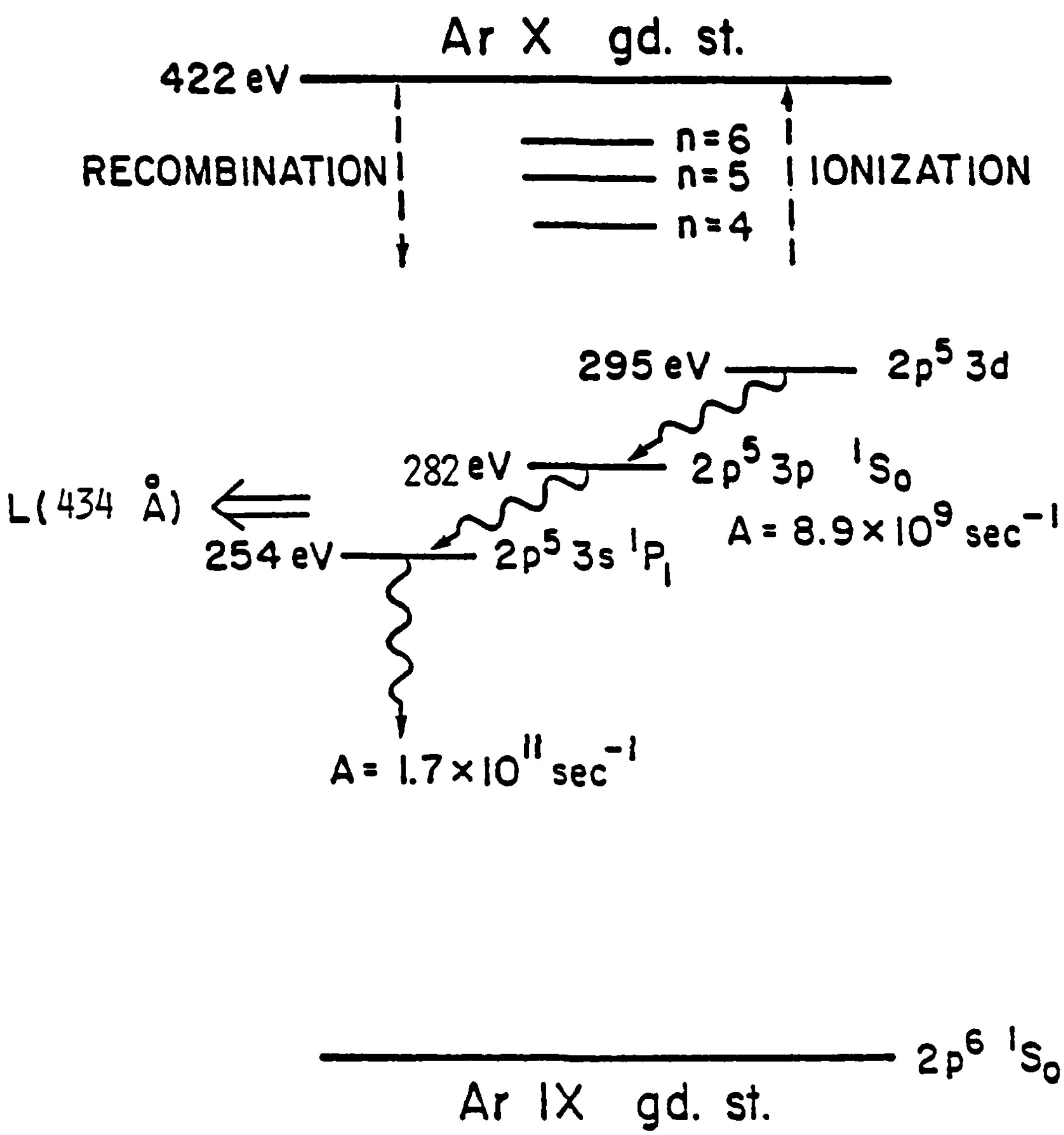

Fig. 1 Abbreviated energy level diagram for neonlike argon.

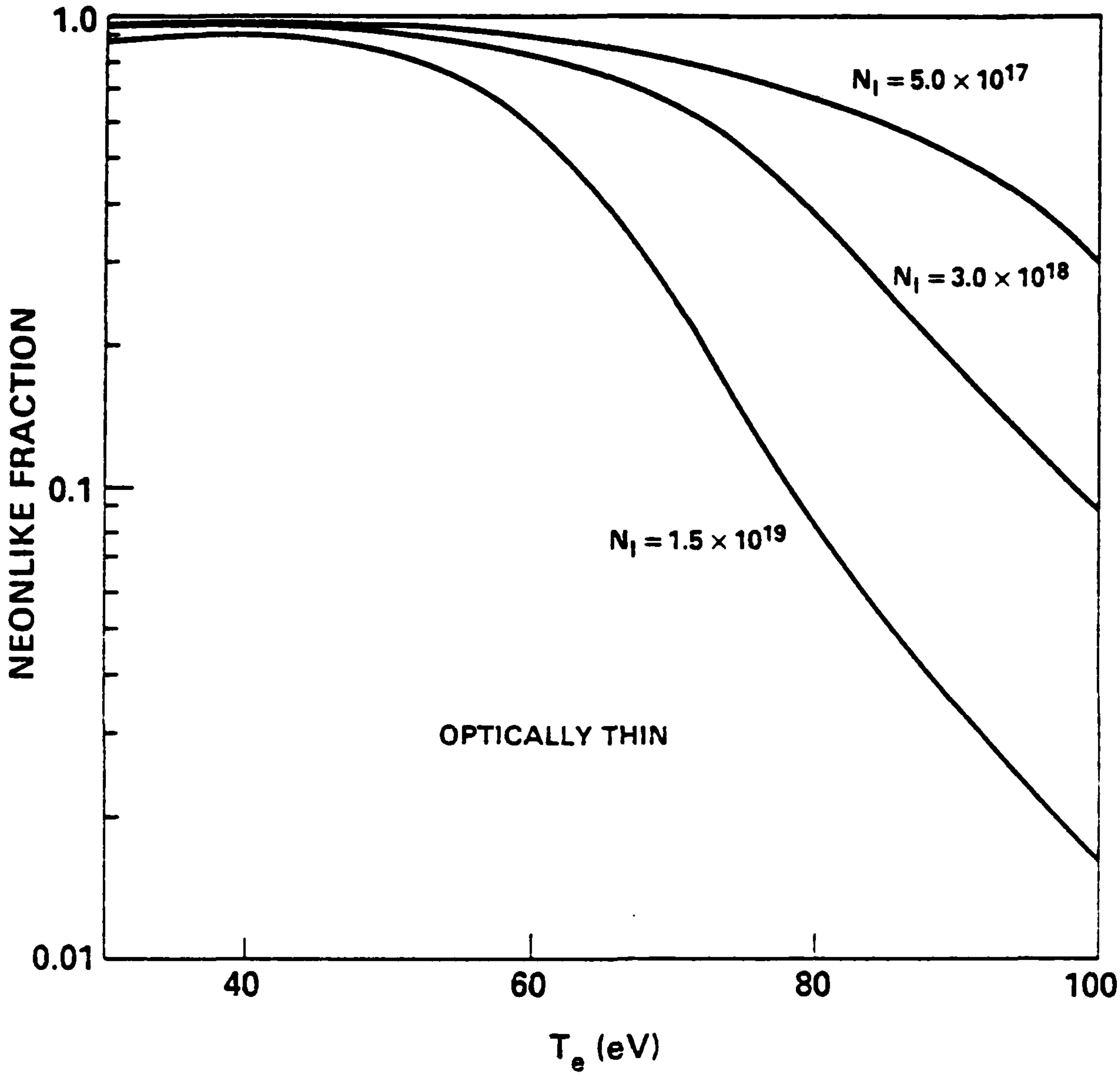

Fig. 2 Neonlike ion fraction as a function of temperature. Plasma assumed optically thin.

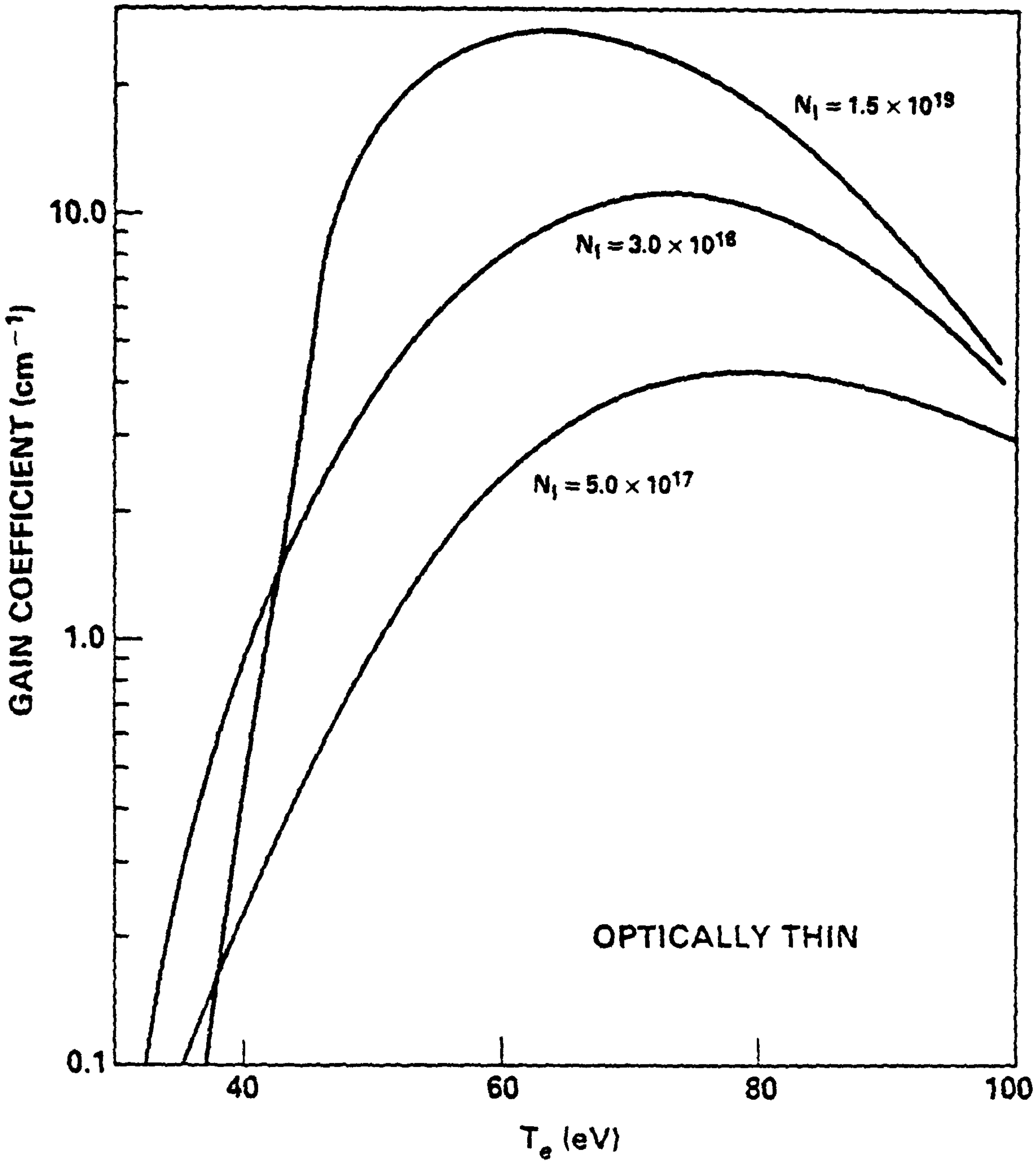

Fig. 3 Gain coefficient as a function of temperature for the 3p-3s transition at 434 Å. Plasma is assumed optically thin.

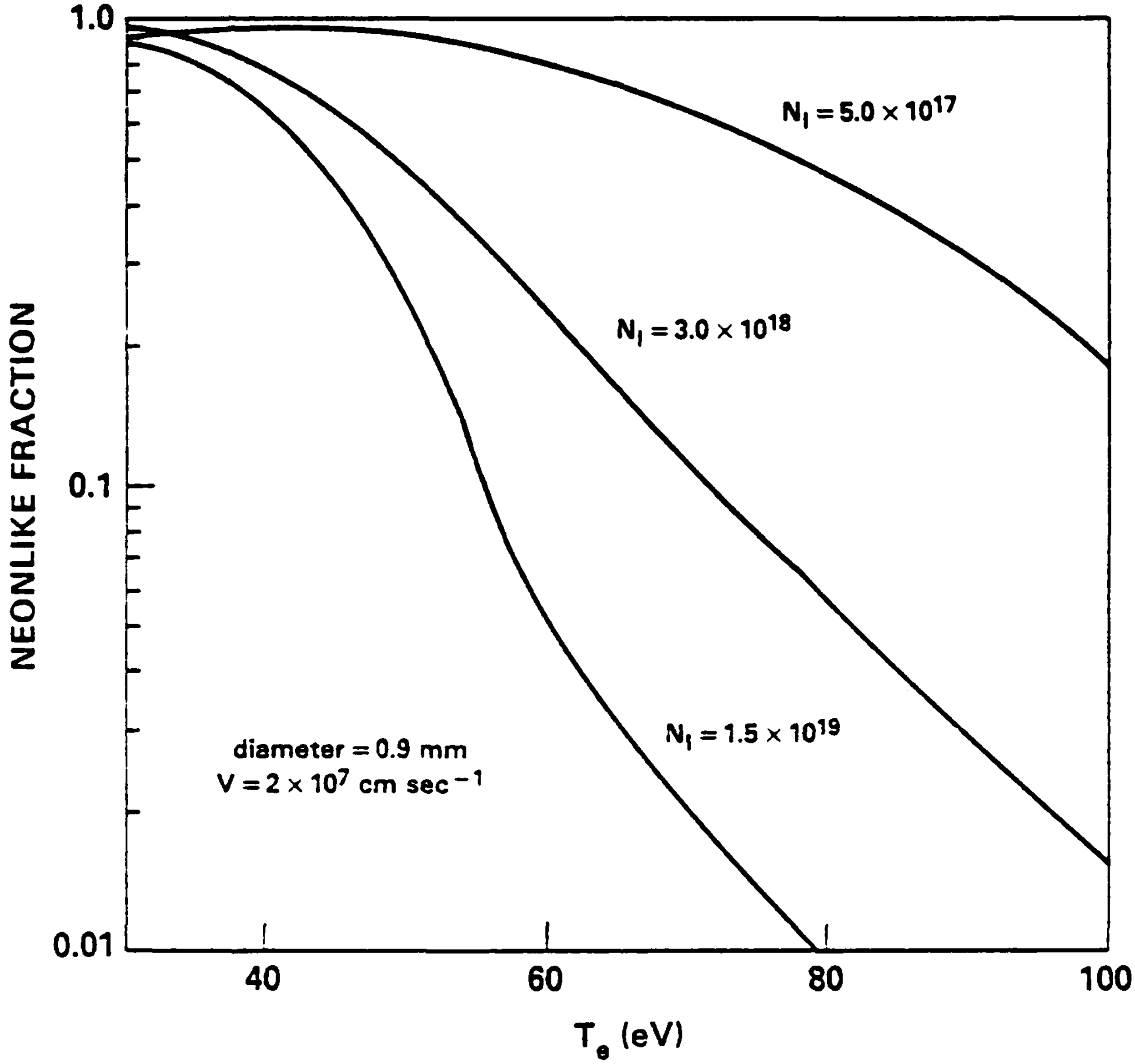

Fig. 4 Neonlike ion fraction as a function of temperature - Opaque case.

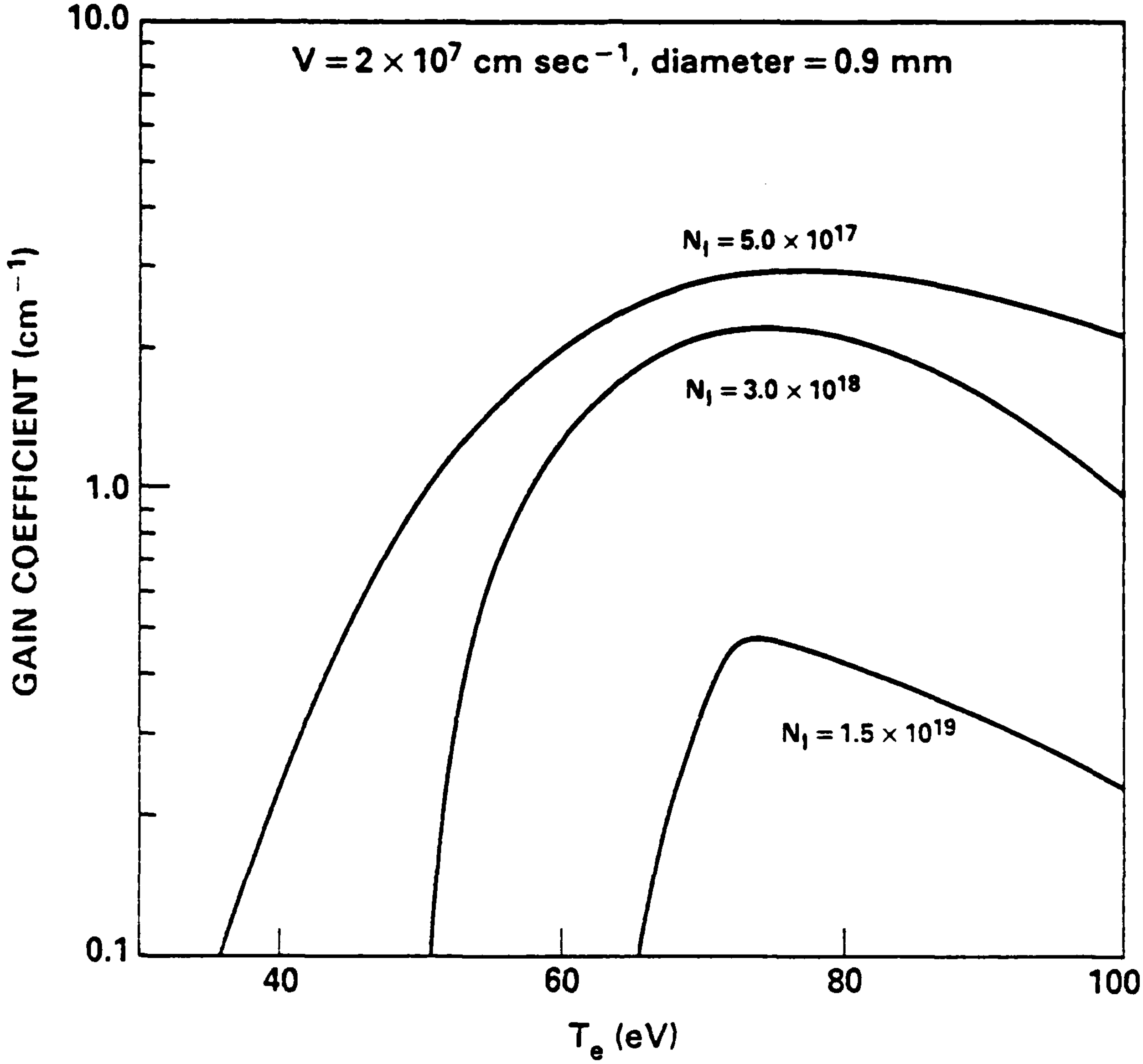

Fig. 5 Gain coefficient as a function of temperature - Opaque case.

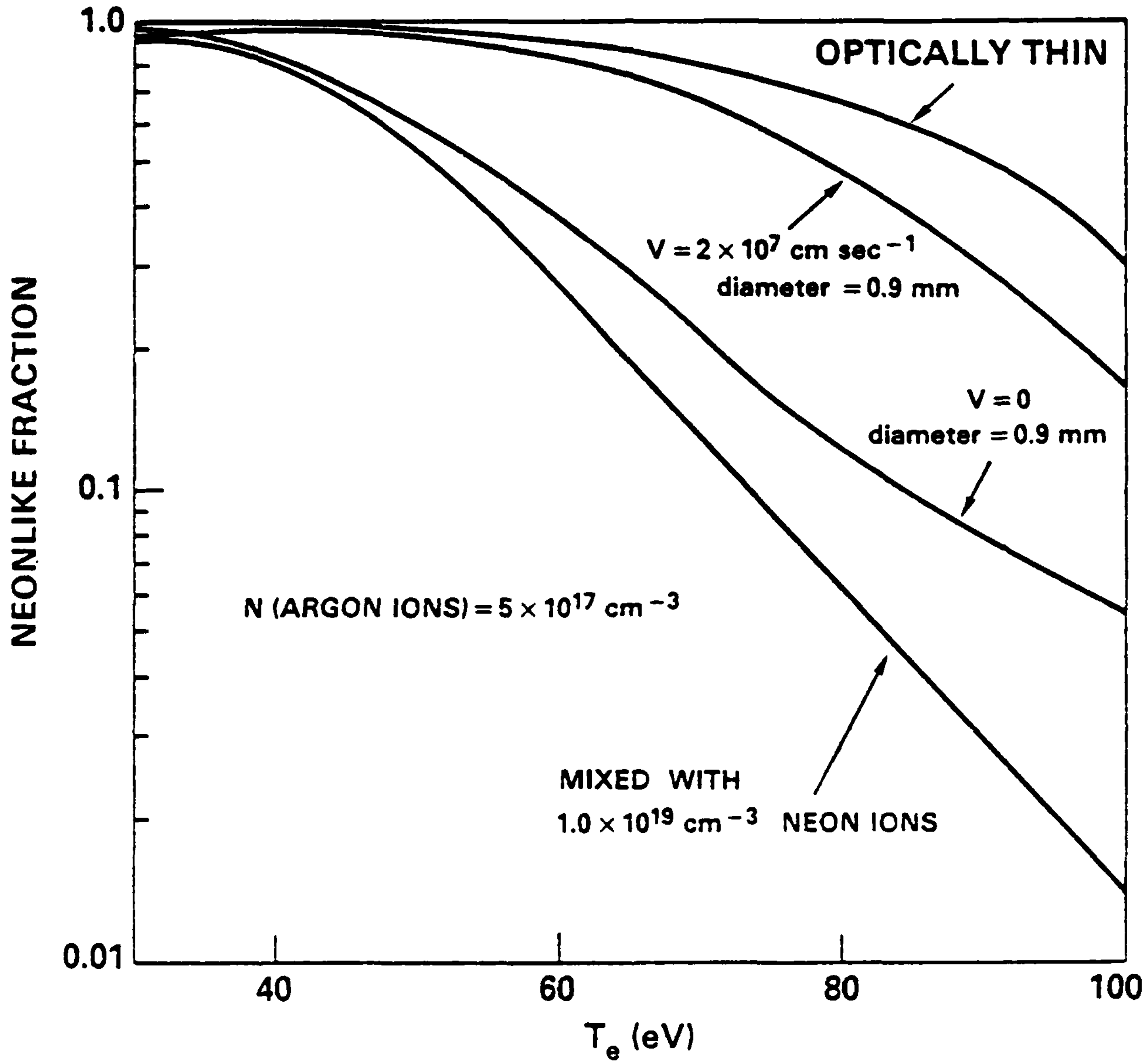

Fig. 6 Neonlike ion fraction as a function of temperature - Mixed velocity and opacity case.

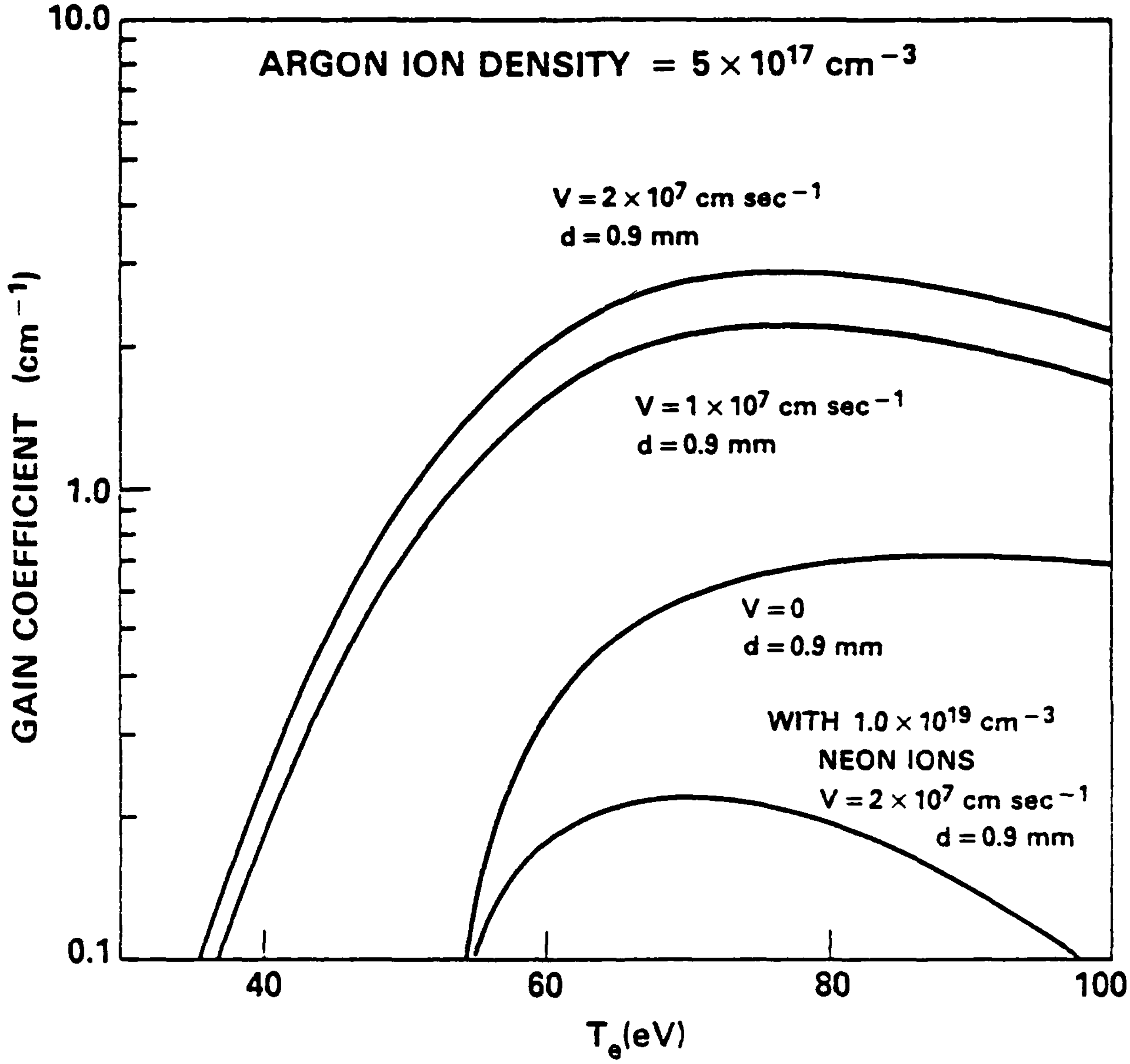

Fig. 7 Gain coefficient as a function of temperature - Mixed velocity and opacity case.

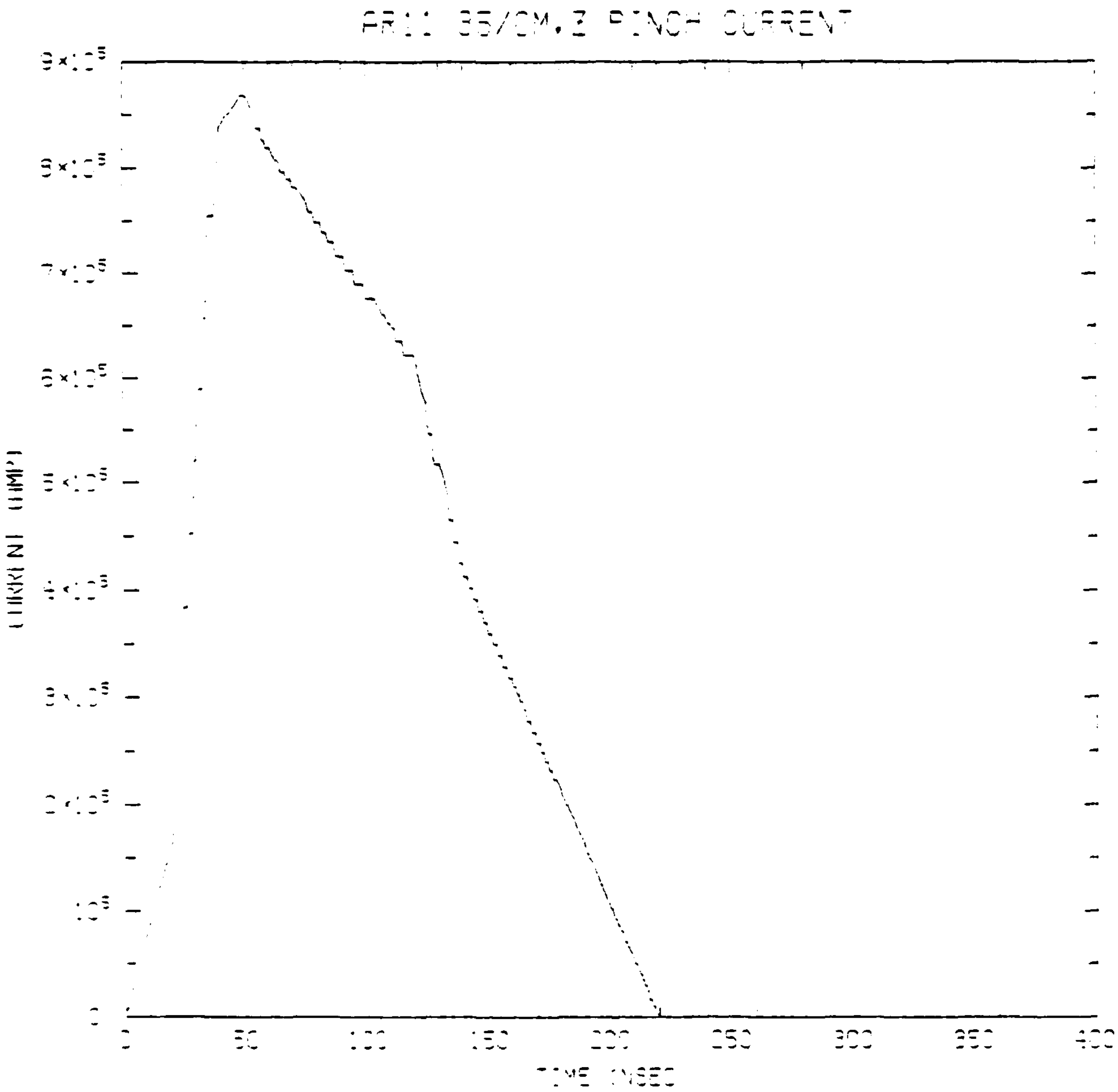

Fig. 3 Current waveform as a function of time.

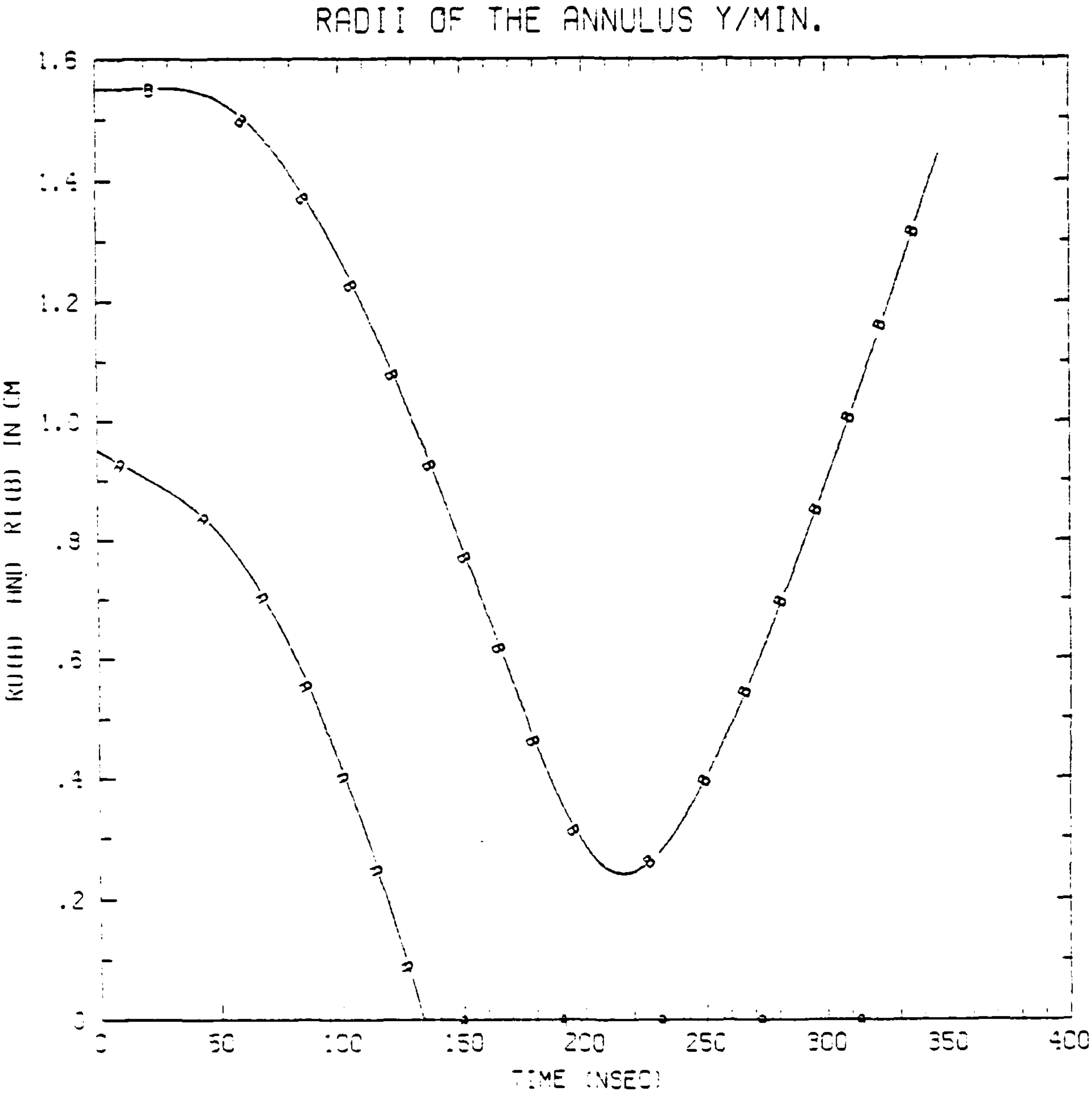

Fig. 9 Inner and outer shell radius as a function of time.

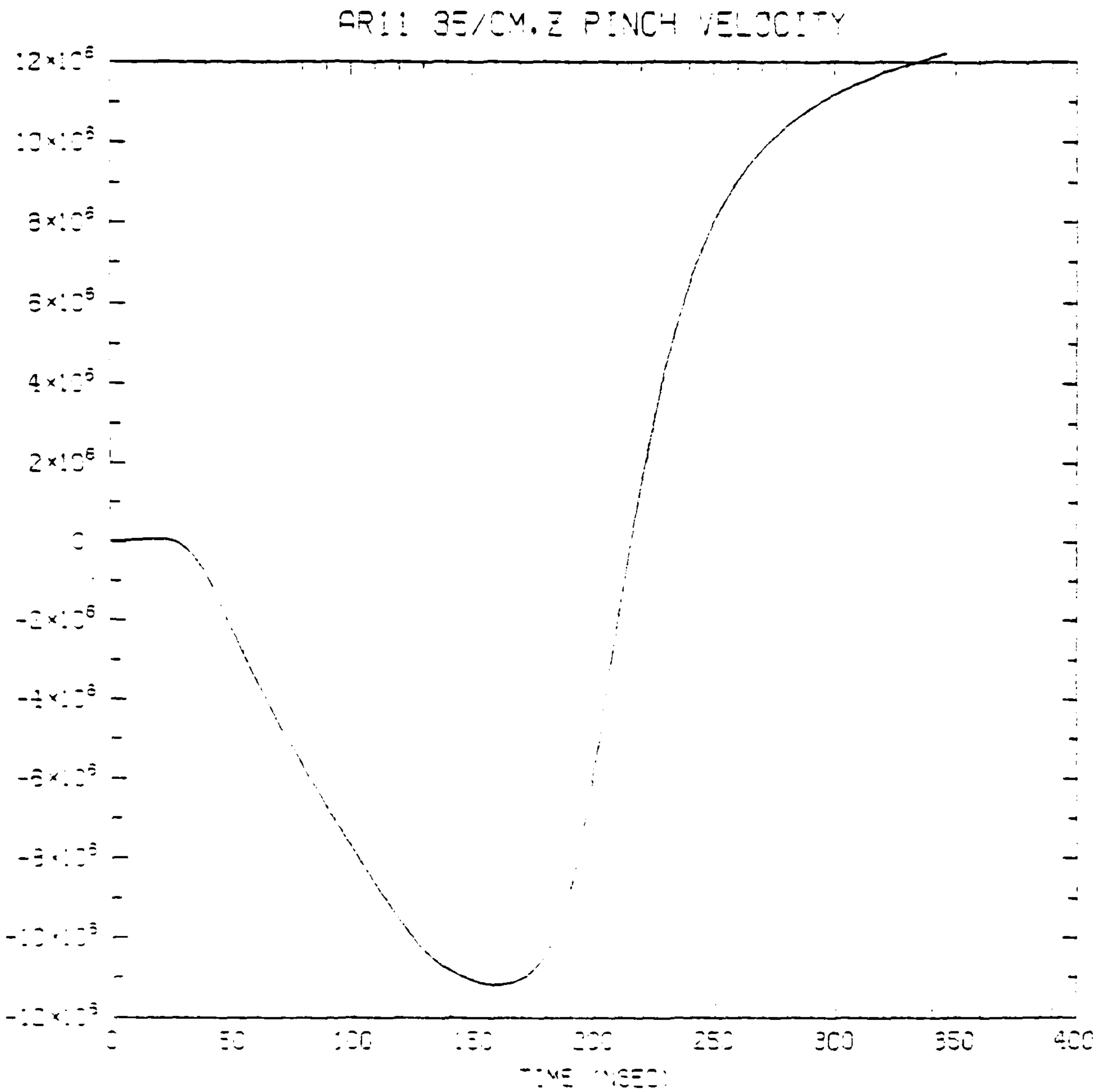

Fig. 10 Implosion velocity as a function of time.

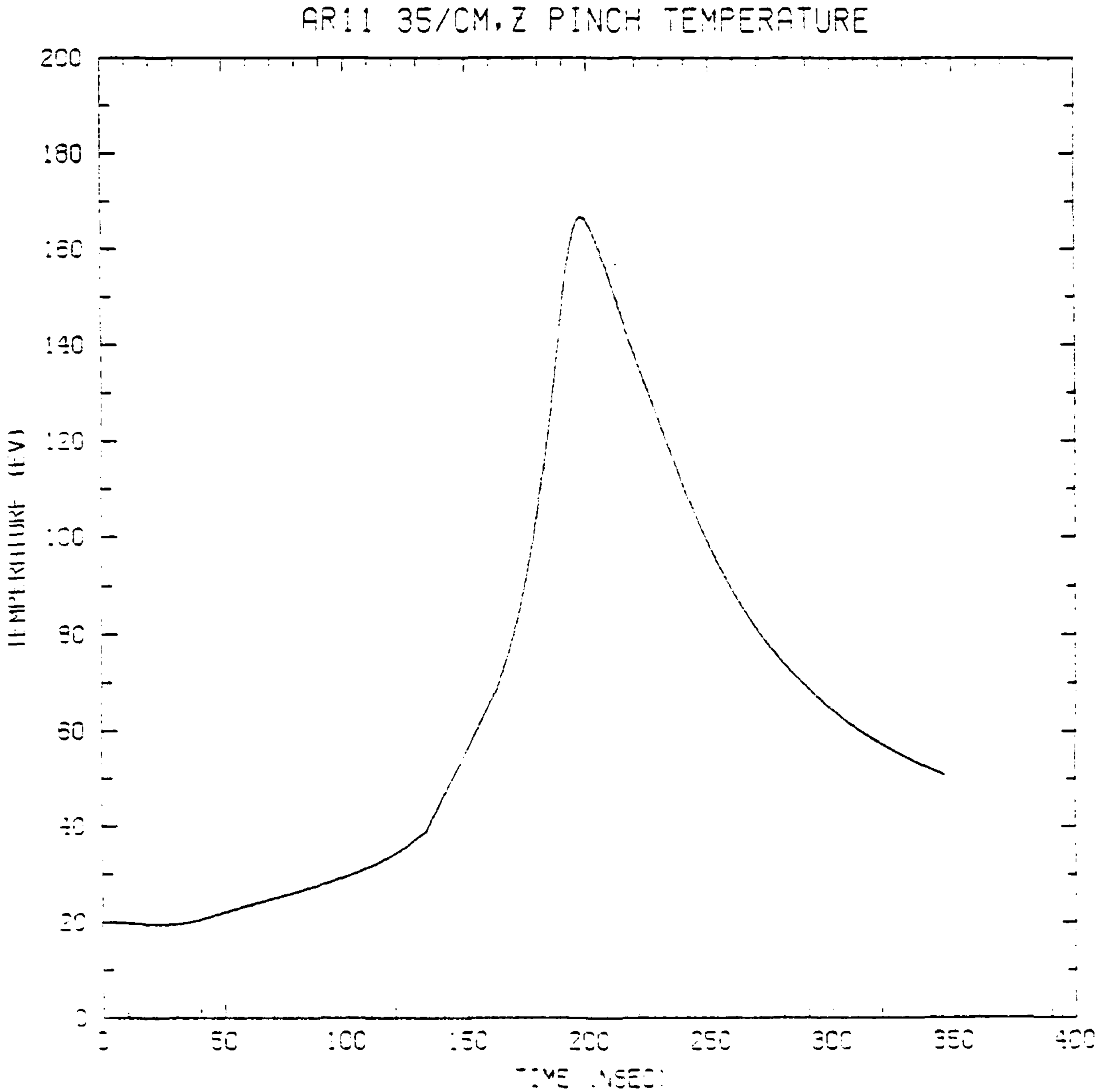

Fig. 11 Temperature as a function of time.

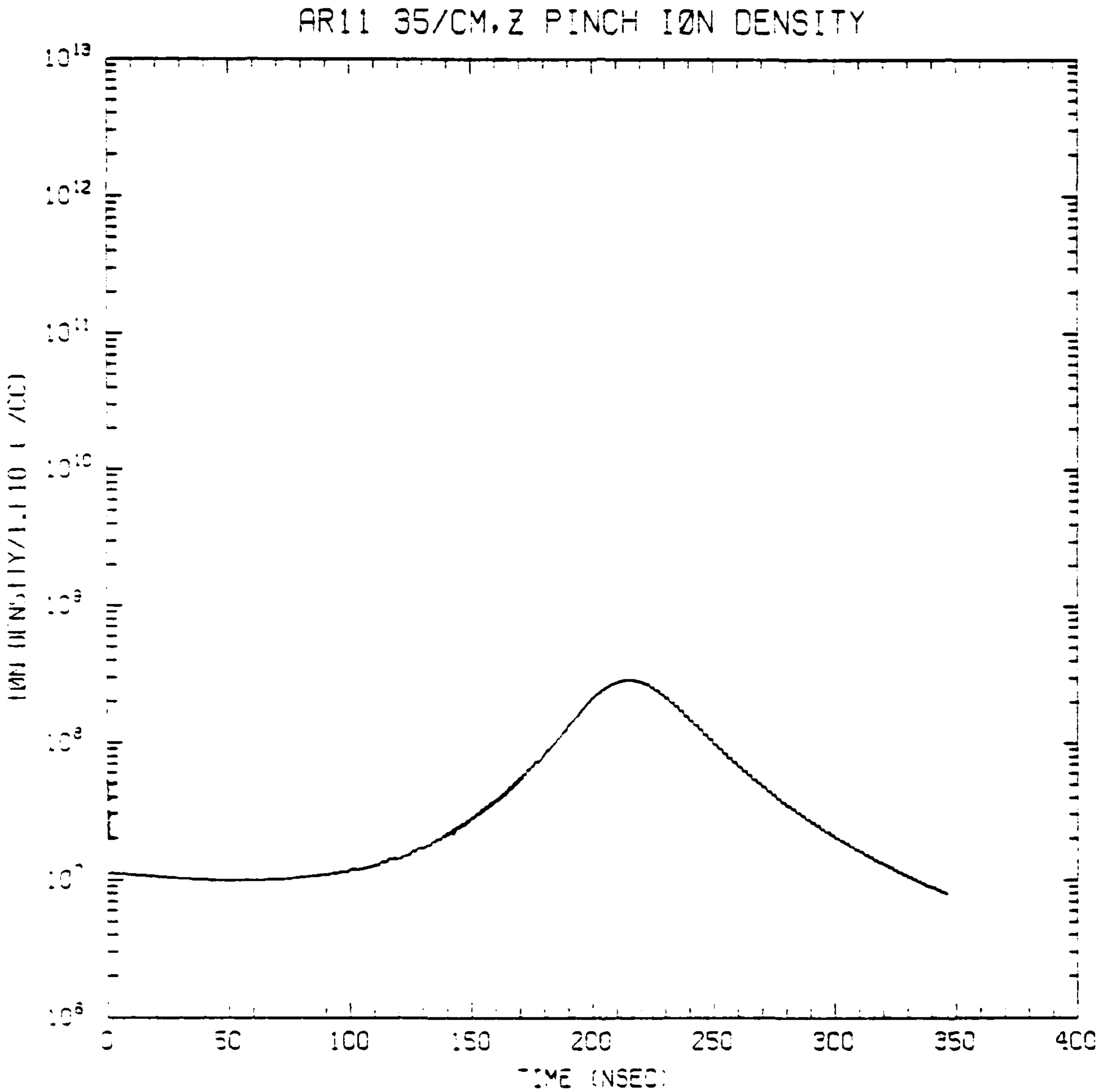

Fig. 12 Ion density as a function of time.

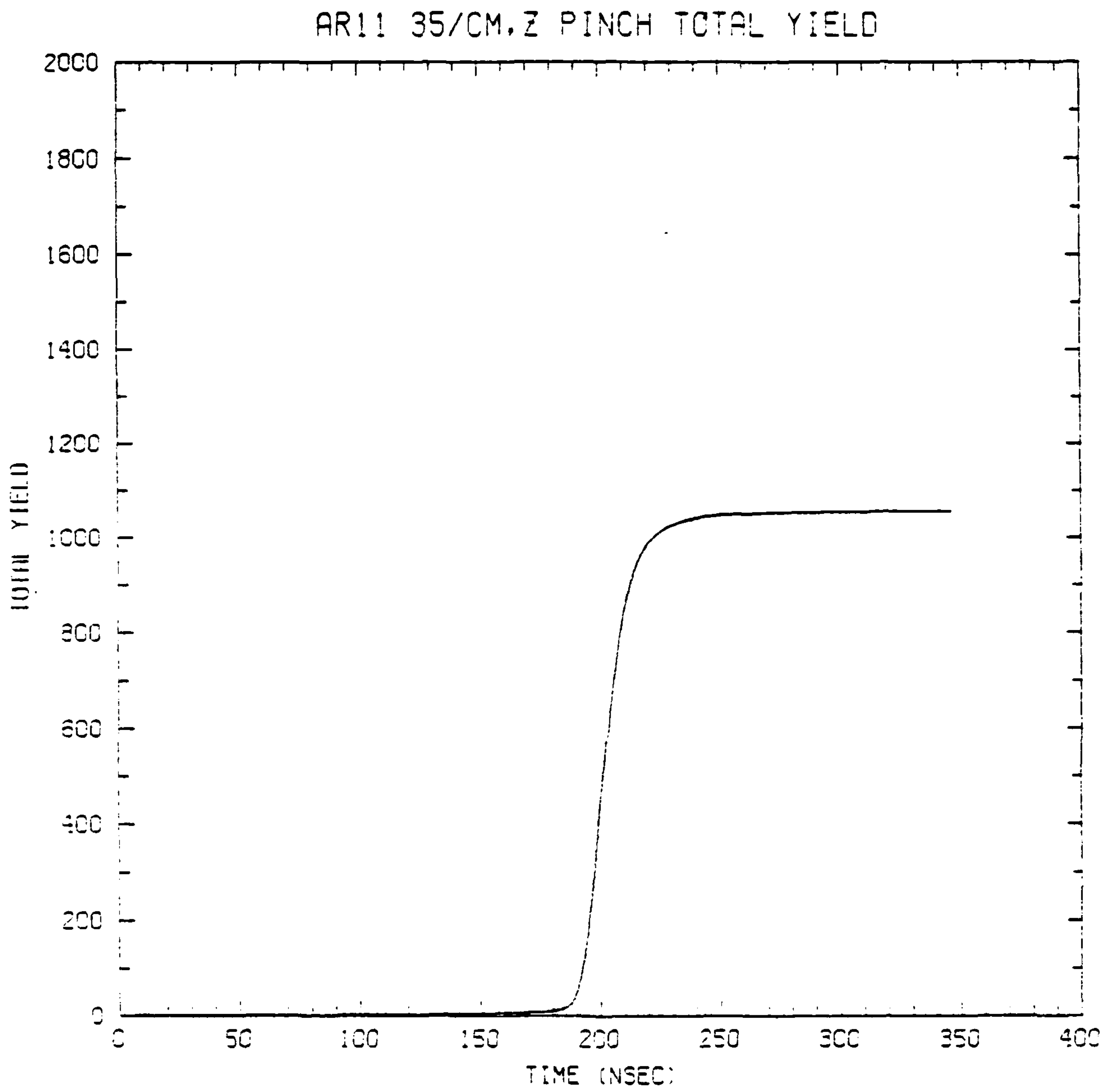

Fig. 13 Total radiative yield (joules) as a function of time.

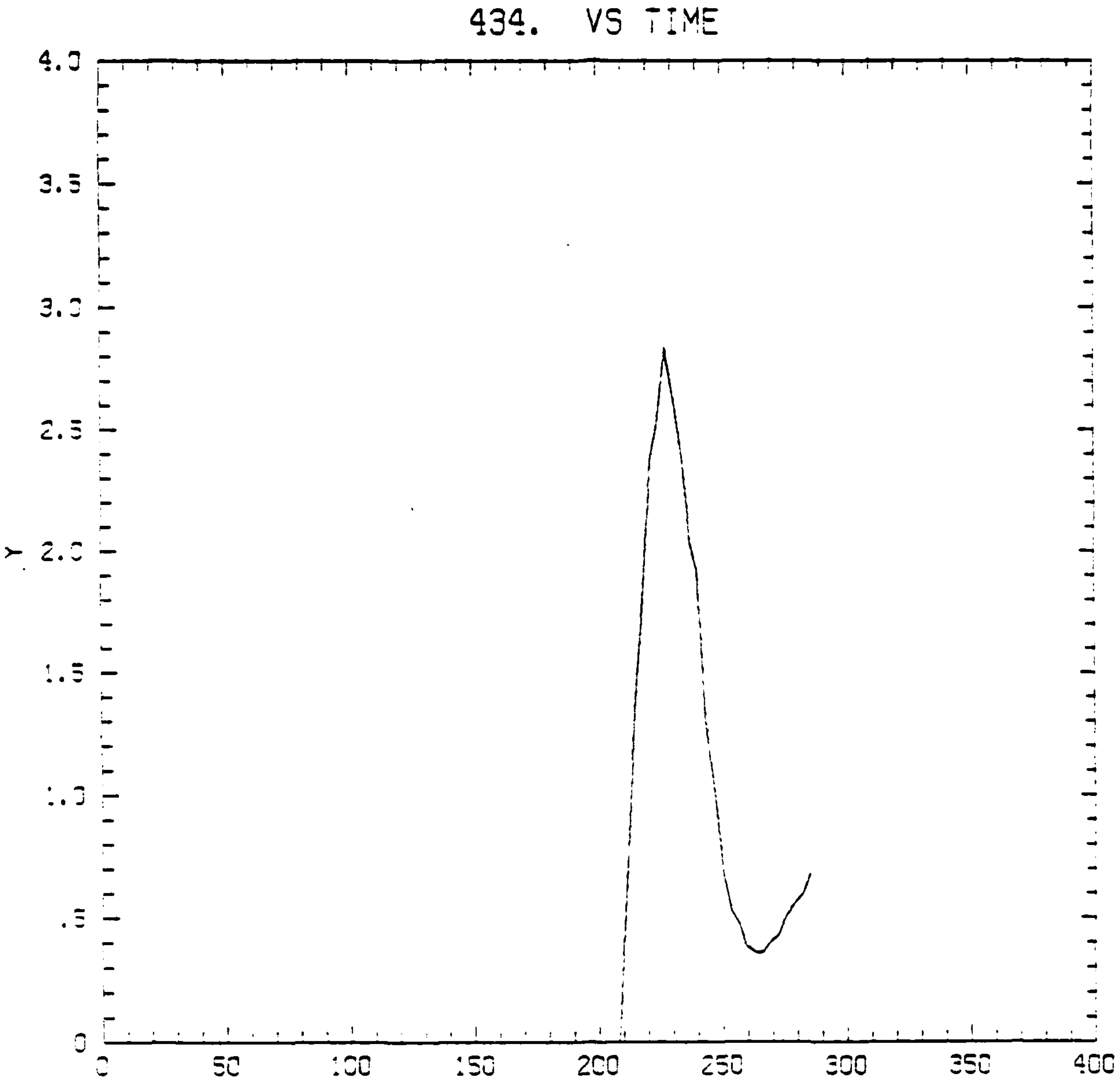

Fig. 14 Gain coefficient at 434 Å as a function of time.

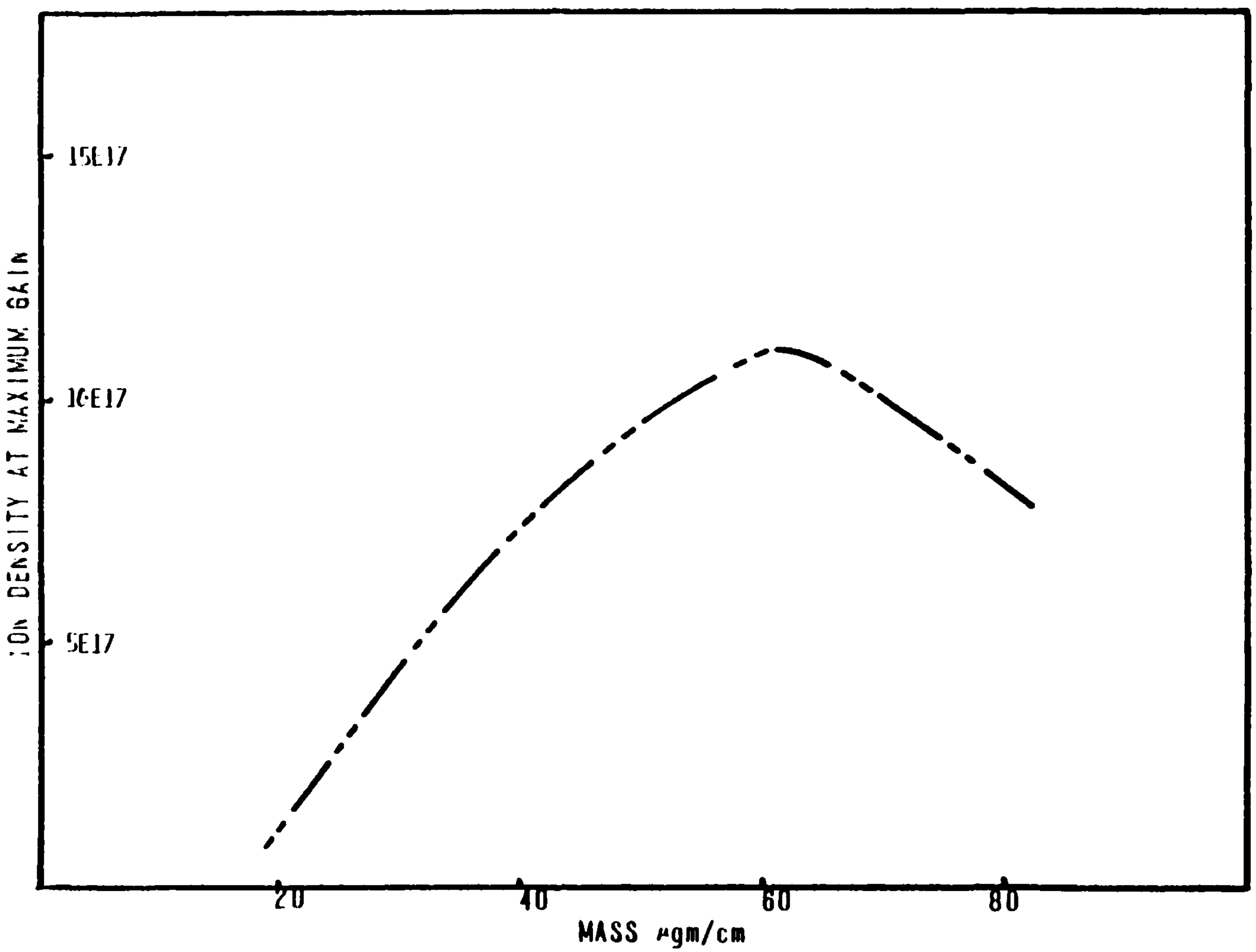

Fig. 15 Ion density at maximum gain as a function of mass per unit length.

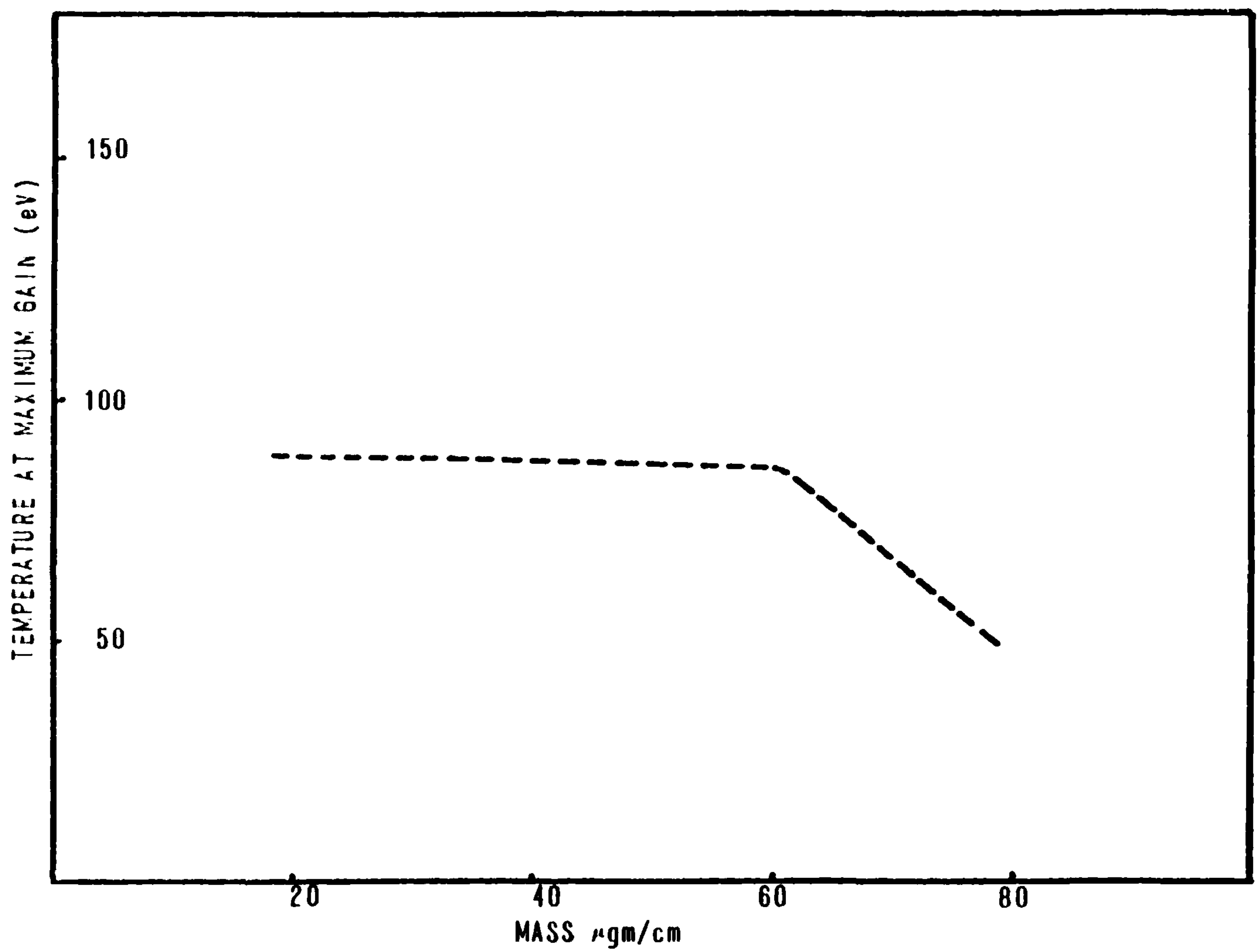

Fig. 16 Temperature at maximum gain as a function of mass per unit length.

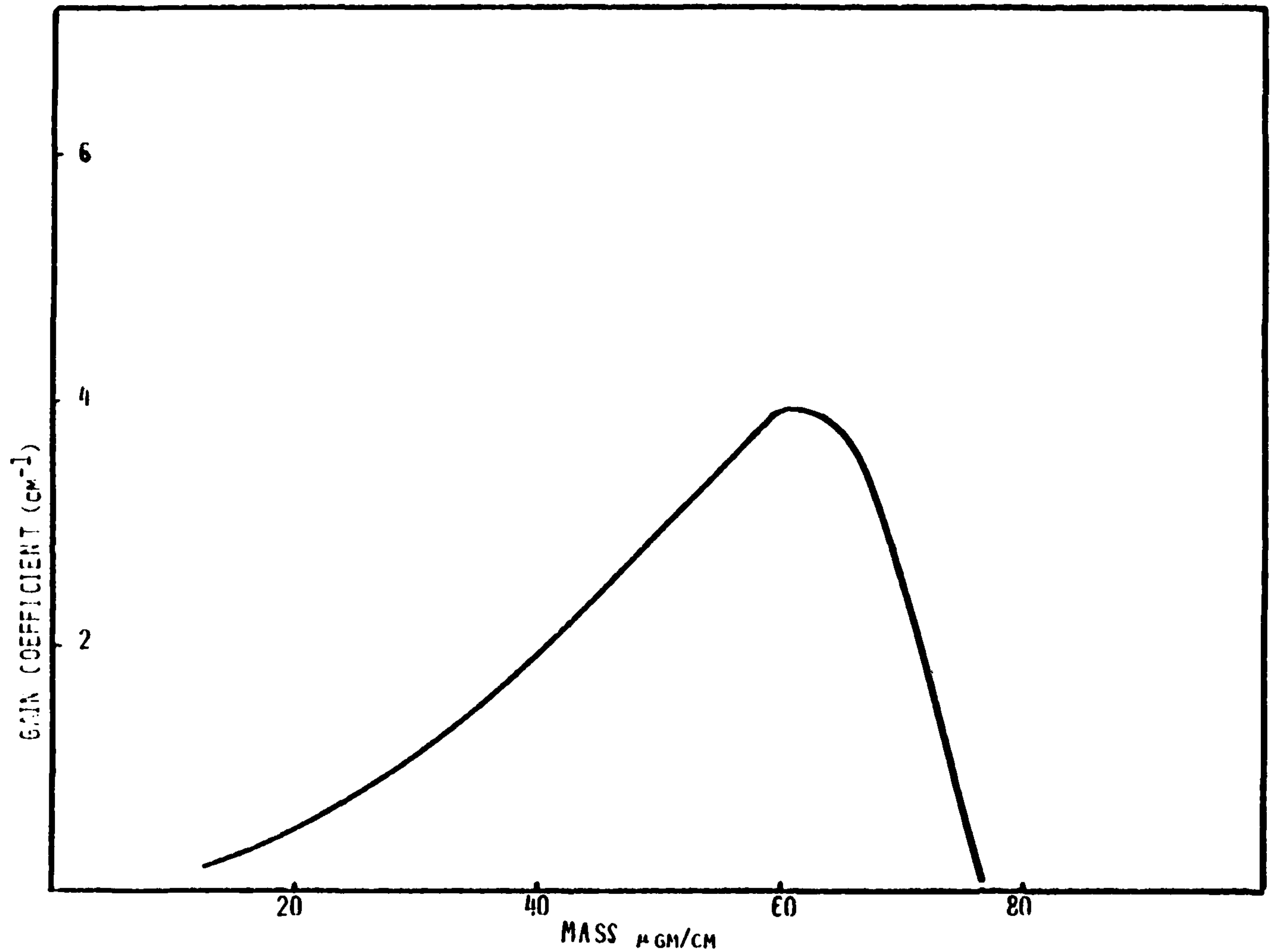

Fig. 17 Gain coefficient at 434 Å as a function of mass per unit length.

References

1. D. Jacoby, G. J. Pert, L. D. Shorrock, and G. L. Tallents, J. Phys. B 15, 3557 (1982).

2. M. D. Rosen, et al., Phys. Rev. Lett. 54, 106 (1985).

3. D. L. Matthews, et al., Phys. Rev. Lett. 54, 110 (1985).

4. S. Suckewer, et al., Phys. Rev. Lett. 55, 1753 (1985).

5. J. F. Seely, et al., Optics Commun. 54, 289 (1985).

6. R. Clark, J. Davis, and F. Cochran, Phys. Fluids, May (1986).

7. 3rd International Conference on Radiative Properties of Hot Dense Matter, Williamsburg, Va. (Oct. 1985).

8. F. C. Young, S. J. Stephanakis, et al., Bull. APS 30, 1389 (1985).

9. J. P. Apruzese and J. Davis, Phys. Rev. A 31, 2976 (1985).

10. V. V. Sobolev, Sov. Astron. 1, 678 (1957).

11. J. Shearer, Phys. Fluids 19, 1426 (1976).

12. J. Davis and K. G. Whitney, JAP 47, 1426 (1975) and D. Duston and J. Davis, Phys. Rev. A 21, 1664 (1980).

DISTRIBUTION LIST

Assistant to the Secretary of Defense Atomic Energy Washington, D.C. 20301 ATTN: Executive Assistant	1 Copy
Defense Technical Information Center Cameron Station 5010 Duke Street Alexandria, Va 22314	2 copies
Director Defense Intelligence Agency Washington, D.C. 20301 ATTN: DT-1B R. Rubenstein	1 Copy
Director Defense Nuclear Agency Washington, D.C. 20305	
ATTN: DDST	1 copy
ATTN: TITL	4 copies
ATTN: RAEV	1 copy
ATTN: STVI	1 copy
Commander Field Command Defense Nuclear Agency Kirtland AFB, New Mexico 87115 ATTN: FCPR	1 Copy
Chief Field Command Livermore Division Department of Defense P.O. Box 308 Livermore, CA 94550 ATTN: FCPRL	1 Copy
Director Joint Strat TGT Planning Staff Offutt AFB Omaha, Nebraska 68113 ATTN: JLKS	1 Copy
Undersecretary of Defense for RSCH and ENGRG Department of Defense Washington, D.C. 20301 ATTN: Strategic and Space Systems (OS)	1 Copy

Deputy Chief of Staff for RSCH DEV and ACQ | 1 Copy
Department of the Army
Washington, D.C. 20301
ATTN: DAMA-CSS-N

Commander | 1 copy each
Harry Diamond Laboratories
Department of the Army
2800 Powder Mill Road
Adelphi, MD 20783
ATTN: DELHD-N-NP
ATTN: DELHD-R J. Rosado
ATTN: DELHD-TA-L (Tech. Lib.)

U.S. Army Missile Command
Redstone Scientific Information Center | 3 Copies
Attn: DRSMI-RPRD (Documents)
Redstone Arsenal, Alabama 35809

Commander | 1 copy
U.S. Army Missile Command
Redstone Arsenal, Alabama 35898
ATTN: DRCPM-PE-EA

Commander
U.S. Army Nuclear and Chemical Agency
7500 Backlick Road | 1 copy
Building 2073
Springfield, VA 22150
ATTN: Library

Commander | 1 Copy
Naval Intelligence Support Center
4301 Suitland Road, Bldg. 5
Washington, D.C. 20390
ATTN: NISC-45

Commander | 1 Copy
Naval Weapons Center
China Lake, California 93555
ATTN: Code 233 (Tech. Lib.)

Officer in Charge | 1 Copy each
White Oak Laboratory
Naval Surface Weapons Center
Silver Spring, Md. 20910
ATTN: Code R40
ATTN: Code F31

Director of Research
U.S. Naval Academy
Annapolis, MD 21402 | 2 Copies

Air Force Weapons Laboratory
Kirtland AFB, New Mexico 87117
ATTN: SUL
ATTN: CA
ATTN: APL
ATTN: Lt. Col Generosa

1 Copy each

Deputy Chief of Staff
Research, Development and Accounting
Department of the Air Force
Washington, D. C. 20330
ATTN: AFRDQSM

1 Copy

Commander
U.S. Army Test and Evaluation Command
Aberdeen Proving Ground, MD 21005
ATTN: DRSTE-EL

1 Copy

AVCO Research and Systems Group
201 Lowell Street
Wilminton, MA 01887
ATTN: Library A830

1 Copy

BDM Corporation
7915 Jones Branch Drive
McLean, Virginia 22101
ATTN: Corporate Library

1 Copy

Berkeley Research Associates
P.O. Box 983
Berkeley, CA 94701
ATTN: Dr. Joseph Workman

1 Copy

Berkeley Research Associates
P.O. Box 852
5532 Hempstead Way
Springfield, VA 22151
ATTN: Dr. Joseph Orens

1 Copy each

Boeing Company
P. O. Box 3707
Seattle, WA 98134
ATTN: Aerospace Library

1 Copy

The Dikewood Corporation
1613 University Bldv., N.E.
Albuquerque, New Mexico 87110
ATTN: L. Wayne Davis

1 Copy

General Electric Company
Space Division
Valley Forge Space Center
P. O. Box 8555
Philadelphia, PA 19101
ATTN: J. Peden

1 Copy

General Electric Company - Tempo
Center for Advanced Studies
816 State Street
P.O. Drawer QQ
Santa Barbara, CA 93102
ATTN: DASIAC

1 Copy

Institute for Defense Analyses
1801 N. Beauregard St.
Alexandria, VA 22311
ATTN: Classified Library

1 Copy

IRT Corporation
P.O. Box 81087
San Diego, CA 92138
ATTN: R. Mertz

1 Copy

JAYCOR
11011 Forreyane Rd.
P.O. Box 85154
San Diego, CA 92138
ATTN: E. Wenaas
F. Felbar

1 Copy

JAYCOR
205 S. Whiting Street, Suite 500
Alexandria, VA 22304
ATTN: R. Sullivan

1 Copy

KAMAN Sciences Corp.
P. O. Box 7463
Colorado Springs, CO 80933
ATTN: Library

1 copy each

Lawrence Livermore National Laboratory
University of California
P.O. Box 808
Livermore, California 94550
Attn: DOC CDN for L-153
Attn: DOC CDN for L-47 L. Wouters
Attn: DOC CDN for Tech. Infor. Dept. Lib.

1 copy each

Lockheed Missiles and Space Co., Inc.
P. O. Box 504
Sunnyvale, CA 94086
Attn: S. Taimity
Attn: J.D. Weisner

1 copy each

Lockheed Missiles and Space Co., Inc.
3251 Hanover Street
Palo Alto, CA 94304
Attn: J. Perez

1 Copy

Maxwell Laboratory, Inc.
9244 Balboa Avenue
San Diego, CA 92123
ATTN: A. Kolb
ATTN: M. Montgomery
ATTN: J. Shannon

1 Copy each

McDonnell Douglas Corp.
5301 Bolsa Avenue
Huntington Beach, CA 92647
ATTN: S. Schneider

1 Copy

Mission Research Corp.
P. O. Drawer 719
Santa Barbara, CA 93102
ATTN: C. Longmire
ATTN: W. Hart

1 Copy each

Mission Research Corp.-San Diego
5434 Ruffin Rd.
San Diego, California 92123
ATTN: Victor J. Van Lint

1 Copy

Northrop Corporation
Northrop Research and Technology Center
1 Research Park
Palos Verdes Peninsula, CA 90274
ATTN: Library

1 Copy

Northrop Corporation
Electronic Division
2301 120th Street
Hawthorne, CA 90250
ATTN: V. Damarting

1 Copy

Physics International Company
2700 Merced Street
San Leandro, CA 94577
ATTN: M. Krishnan
ATTN: C. Gilman
ATTN: S. Wong

1 Copy each

R and D Associates
P.O. Box 9695
Marina Del Rey, CA 90291
ATTN: W. Graham, Jr.
ATTN: P. Haas

1 Copy each

Sandia National Laboratories P.O. Box 5800 Albuquerque, New Mexico 87115 ATTN: Doc Con For 3141 ATTN: D. McDaniel ATTN: P. VanDevender ATTN: K. Matzen, Code 4247	1 copy each
Science Applications, Inc. P. O. Box 2351 La Jolla, CA 92038 ATTN: R. Beyster	1 copy
Spire Corporation P. O. Box D Bedford, MA 01730 ATTN: R. Little	1 copy
SRI International 333 Ravenswood Avenue Menlo Park, CA 94025 ATTN: S. Dairiki	1 copy
S-CUBED P. O. Box 1620 La Jolla, CA 92038 ATTN: A. Wilson	1 copy
Director Strategic Defense Initiative Organization 1717 H Street Pentagon 20301-7100 ATTN: DE Lt. Col Richard Gullickson/DEO IST Dr. Dwight Duston ATTN: IST Dr. J. Ionson	1 copy each
Texas Tech University P.O. Box 5404 North College Station Lubbock, TX 79417 ATTN: T. Simpson	1 copy
TRW Defense and Space Systems Group One Space Park Redondo Beach, CA 90278 ATTN: Technical Information Center	1 Copy

Naval Research Laboratory
Plasma Radiation Branch
Washington, D.C. 20375

Code 4720 - 50 Copies
Code 4700 - 26 Copies
Code 2628 - 20 Copies
Code 1220 - 1 Copy

END
FILMED

6-86

DTIC